Thermal conductivity of $(Er_{1-x}Y_x)_2Ti_2O_7$ pyrochlore oxide solid solutions

Craig Bryan,[1] Catherine A. Whitman,[1,2] Michel B. Johnson,[2] John F. Niven,[3] Patrick Murray,[1] Alex Bourque,[1,2] Hanna A. Dąbkowska,[4] Bruce D. Gaulin,[4,5] and Mary Anne White[1,2,3,*]

[1]*Department of Chemistry, Dalhousie University, Halifax, Nova Scotia, Canada B3H 4R2*

[2]*Institute for Research in Materials, Dalhousie University, Halifax, Nova Scotia, Canada B3H 4R2*

[3]*Department of Physics and Atmospheric Science, Dalhousie University, Halifax, Nova Scotia, Canada B3H 4R2*

[4]*Brockhouse Institute for Materials Research, McMaster University, Hamilton, Ontario, Canada L8S 4M1*

[5]*Department of Physics and Astronomy, McMaster University, Hamilton, Ontario, Canada L8S 4M1*

(Received 2 May 2012; revised manuscript received 4 July 2012; published 14 August 2012)

The thermal conductivities of pyrochlore oxide solid solutions of general formula $(Er_{1-x}Y_x)_2Ti_2O_7$ with $0 \leqslant x \leqslant 1$ have been determined for high-quality single crystals aligned along the [110] direction, over the temperature range from 3 to 300 K. $Er_2Ti_2O_7$ and $Y_2Ti_2O_7$ are isostructural and Er^{3+} and Y^{3+} are within 1% in size, but differ by a factor of about 2 in mass. Therefore, this system allows a clear test of the influence of mass of dopant on thermal conductivity, while controlling for other factors such as dopant size and sample purity. Although $Y_2Ti_2O_7$ has a higher thermal conductivity than $Er_2Ti_2O_7$ at $T = 300$ K, from 3 to 200 K their relative thermal conductivities reverse. Furthermore, we observe significant decrease in thermal conductivity upon doping $Er_2Ti_2O_7$ with Y^{3+} ions, showing definitively that, in the temperature range from about 3 to 300 K, the impurity scattering effect of the lighter Y^{3+} ions is the predominant limiter of the thermal conductivity. This conclusion is supported by the finding that the phonon mean free path of the doped compounds decreases with increased dopant concentrations, increasing again as pure $Y_2Ti_2O_7$ is approached.

DOI: 10.1103/PhysRevB.86.054303 PACS number(s): 65.40.−b

I. INTRODUCTION

Pyrochlore oxides have cubic structures with the general formula $A_2B_2O_7$, with a structure analogous to the mineral pyrochlore. They have been of recent interest due to their exceptional properties,[1] including high resistance to radiation,[2] magnetic geometric frustration,[3] and inherently low thermal conductivity.[4,5]

As rigid structures, the thermal conductivity of pyrochlores cannot be lowered by the addition of rattling atoms,[6,7] or by the presence of low-frequency optical modes that can interact with heat-carrying acoustic modes.[8,9] However, the thermal conductivity of pyrochlores can be lowered by other means, including high mean atomic mass, weak nondirectional bonding, and extensive disorder (either structural or due to doping).[10] The combination of low thermal conductivity with high melting point makes some pyrochlores useful for new thermal barrier materials in applications such as high-speed turbines. Several recent studies have focused on quantifying this low thermal conductivity and reducing it further.[4,5,11–13] In particular, introduction of dopants into the pyrochlore structure can provide point defects in the crystal lattice that reduce the intrinsic phonon mean free path.[14] Generally, as the number density of point defects within a crystal is increased, the phonon mean free path is decreased, and the thermal conductivity is decreased accordingly. Several studies have investigated the thermal conductivity of a series of compounds doped at the A site in the crystal lattice giving the general formula $(A_{1-x}A'_x)_2B_2O_7$.[11–13]

In particular, laser-flash thermal conductivity studies of A-site doped pyrochlores at high temperatures showed that the lowest thermal conductivity occurs at a composition with roughly equal concentrations of dopant and parent ions, that is, $AA'B_2O_7$.[11,12] At compositions closer to the end members $A_2B_2O_7$ or $A'_2B_2O_7$, the thermal conductivity tends to be higher. However, the effect of A-site doping is less significant as the temperature increases.[11–13] At these high temperatures, Umklapp processes, rather than the defect sites, limit the phonon mean free path.[14] Thus, as the temperature increases, the effect of dopant ions on the phonon mean free path is less significant.

The influences of the size and mass of the dopant ion in A-site doping studies of pyrochlores have been investigated recently by molecular dynamics simulations.[13] That study considered three different A-site dopants in the same parent compound, $Gd_2Zr_2O_7$. The effect of introducing a dopant ion similar in size and mass to the parent ion was tested using Sm^{3+} as the dopant. From the simulations, very little change in thermal conductivity was observed with that doping, even at high concentrations of Sm^{3+} dopant ions.[13] The effect of introducing a dopant of significantly less mass compared to the parent ion was investigated using Y^{3+}. A slight lowering of the thermal conductivity was observed in the simulations, and attributed to the phonon-scattering effect of the dopant (lowering κ), competing with the significantly higher thermal conductivity of pure $Y_2Zr_2O_7$.[13] Lastly, the effect of using a dopant ion with a significantly larger size was explored using La^{3+} as the dopant ion. The resultant series of compounds $(La_{1-x}Gd_x)_2Zr_2O_7$ gave the most significant decrease (up to about 20% at room temperature) in thermal conductivity with doping.[13]

Previous experimental A-site doping studies were focused on pyrochlores as thermal barrier materials and therefore concentrated on high temperature, typically 300 to 900 K,[11–13] where Umklapp processes are the dominant phonon scattering mechanism.[14] Thus, it could be anticipated that the effect of doping on thermal conductivity could be more significant at lower temperatures, where scattering due to Umklapp pro-

cesses is less important. The present study examines the effects of *A*-site doping on thermal conductivity at temperatures below 300 K for a series of $(Er_{1-x}Y_x)_2Ti_2O_7$ pyrochlores. This is an excellent solid solution test system because the pure end members $Er_2Ti_2O_7$ and $Y_2Ti_2O_7$ are isostructural and have very similar lattice parameters, 10.0869(1) and 10.0949(5) Å, respectively, at room temperature,[15] and Er^{3+} and Y^{3+} ions have very similar radii, 0.890 and 0.900 Å, respectively,[16] but vastly different masses (Er: 167.26 g mol^{-1}; Y: 88.91 g mol^{-1}). The thermal conductivity has been measured here directly, in contrast with earlier measurements of thermal diffusivity which also require knowledge of density and heat capacity.[11,12] Therefore the $(Er_{1-x}Y_x)_2Ti_2O_7$ series examined here allows an accurate test of the conclusion from molecular dynamics simulations that dopant ions with a similar size but different mass give only a small reduction in the thermal conductivity of pyrochlores.[13]

II. EXPERIMENTAL DETAILS

A. Sample preparation

Pure erbium titanate $Er_2Ti_2O_7$ and yttrium titanate $Y_2Ti_2O_7$ and solid solutions of the general formula $(Er_{1-x}Y_x)_2Ti_2O_7$ in quantities of approximately 50 g were synthesized by the solid-state reaction of appropriate ratios of Er_2O_3 (Alfa Aesar, 99.99%) and Y_2O_3 (Sigma-Aldrich, 99.99%) with TiO_2 (Sigma-Aldrich, 99.99%) through ball milling for 5 min (3 times) at 250 rpm. The resultant powder was pressed at 60 MPa for 15 to 20 min to form ceramic rods. The homogeneous polycrystalline rods were annealed at 1350 °C in air to prereact and improve their hardness.

Large single crystals were grown from these polycrystalline rods using the optical floating-zone method.[17,18] Two polycrystalline rods were mounted, one above the other, in a two-mirror image furnace (Canon) with the long axes aligned. The focused light from the halogen lamps heated both tips of the ceramic rods until they formed a molten zone. Molten material was then pulled out of the hot area at the rate of 5 to 6 mm h^{-1} and crystallized. The rods were counter-rotated with various speeds (0 to 30 rpm). The result of this process was 60 to 80 mm long, cylindrical single crystals, 6 to 8 mm in diameter. The same method was used for pure erbium titanate $Er_2Ti_2O_7$, pure yttrium titanate $Y_2Ti_2O_7$, and the solid solutions. The growths were performed in 4 atm of Ar.

For thermal conductivity measurements, an approximately 1 mm thick disk-shape section of crystal was cut such that the [110] lattice vector was perpendicular to the flat face of the disk. This alignment was achieved using x-ray diffraction. The consistent alignment of all the samples avoided any directional effects with regard to thermal conductivity. The disks were then cut into cuboids for thermal conductivity measurements. Gold-plated copper leads were adhered to each cuboid on the faces perpendicular to the [110] lattice vector. Silver-loaded epoxy was used to ensure thermal contact between the sample leads and the sample.

The compositions of the solid solution crystals were determined by wavelength dispersive spectroscopy using electron microprobe analysis (JEOL 8200 electron microprobe). Several samples were taken from the same general area of the single crystal to test for homogeneity. As a further test of homogeneity, the electron beam width on each sample was varied from 1 to 10 μm. The quoted uncertainties in composition (*vide infra*) take all these measurements into account.

For comparison to the thermal conductivity of the aligned single crystals, a polycrystalline sample of $Er_2Ti_2O_7$ was cut from the end of the rod where the sample was a consolidation of randomly aligned polycrystals with grain sizes as small as 10 μm. This sample was prepared in the same manner for thermal conductivity measurements.

B. Thermal conductivity

All thermal conductivity measurements were obtained using a physical property measurement system (PPMS) by Quantum Design. In the PPMS thermal transport probe, one lead was attached to a heater and a hot thermometer and the other lead was attached to a heat sink and a cold thermometer. The sample was heated and a temperature differential of approximately 3% of the absolute temperature of the system was created across the sample. Using the measured heater power and the equilibrium temperature difference between the hot and cold ends of the sample, the raw thermal conductance was measured. A small correction for radiative loss and for heat loss through the shoes was applied. Through the measured geometry of the sample, the thermal conductance was converted to the thermal conductivity.[19] Thermal conductivity measurements were carried out in this manner from ~2 to 300 K under high vacuum ($\leqslant 10^{-4}$ Torr).

The accuracy of the thermal measurements was assessed by measuring the thermal conductivity of a known material. Pyrex® glass was chosen as the standard because its thermal conductivity is well documented[20,21] and is of the same order of magnitude as the samples under investigation. The thermal conductivities of five rods of Pyrex® glass with varying lengths were measured at 300 K using the methods described above. The results for all five samples were within 5% of the literature values for thermal conductivity of Pyrex®glass.[20,21] In addition, the measured thermal conductivity of one sample of Pyrex ® glass was determined from 50 to 300 K, and found to be within ±3% of literature values[20] from 100 to 300 K, ±10% at lower temperatures.

III. RESULTS AND DISCUSSION

A. Thermal conductivity[22]

The thermal conductivities κ of two high-purity single crystals of $Er_2Ti_2O_7$ aligned along the [110] lattice vector and one high-purity polycrystalline sample of $Er_2Ti_2O_7$ were determined over the temperature range 2 to 300 K. Results are shown in Fig. 1.

The two single crystals show very similar thermal conductivity behavior over the temperature range and demonstrate the typical temperature dependence for κ for simple crystalline insulating solids.[14,23,24] The consistency of the thermal conductivity of the two single-crystalline samples is excellent, within 3% of the average at all temperatures.

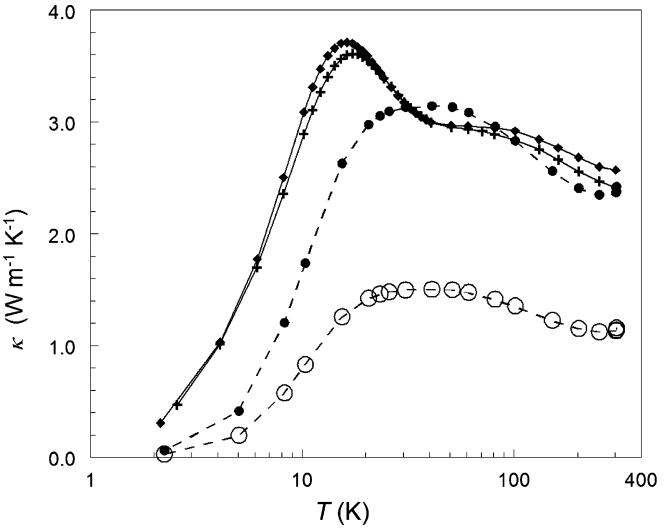

FIG. 1. The experimentally determined thermal conductivities κ of two samples of crystalline $Er_2Ti_2O_7$ (+,♦) along the [110] direction, and one sample of polycrystalline $Er_2Ti_20_7$ (○ as measured; • converted to fully densified, as described in the text), as a function of temperature. The lines are guides for the eye.

The temperature-dependent behavior of the crystals can be understood using the Debye model of thermal conductivity,

$$\kappa = \tfrac{1}{3} C_V v \lambda, \tag{1}$$

where C_V is the heat capacity of the solid per unit volume, v is the speed of the phonons, and λ is the mean free path of the phonons. The speed of the phonons remains nearly constant throughout the temperature range, and the temperature dependence arises from that of the heat capacity and the mean free path. At low temperatures the temperature dependence of the thermal conductivity is governed mostly by the heat capacity of the material, which increases with increasing temperature. The phonon mean free path at these low temperatures is not significantly influenced by temperature-dependent processes such as phonon-phonon interactions. Therefore, at low temperatures the phonon mean free path is related to interruptions of the crystal structure, such as defects or crystal boundaries. As temperature increases, the heat capacity approaches its maximum limiting value, and the phonon mean free path begins to shorten as the probability of phonon-phonon collisions increases.[14] These two trends cause a maximum in the thermal conductivity; increasing the temperature further causes the thermal conductivity to decrease as the phonon mean free path becomes shorter.[14]

The thermal conductivity of the polycrystalline $Er_2Ti_2O_7$ sample is also shown in Fig. 1. The density of the polycrystalline sample is only 60% of that of the single crystal. To consider the effective thermal conductivity of a fully densified polycrystalline sample, the method developed by Klemens[25] was used. These results also are shown in Fig. 1 and allow an unusually direct comparison between the thermal conductivity of a highly purified sample in its single crystalline form and as a polycrystal. The thermal conductivities of single crystalline and fully densified polycrystalline $Er_2Ti_2O_7$ are in excellent agreement (within 5% of the average) for $T > 30$ K. At lower temperatures, where the phonon mean free path is longer and therefore more influenced by the crystallinity, the thermal conductivity for the polycrystalline sample falls below that of the single crystal.

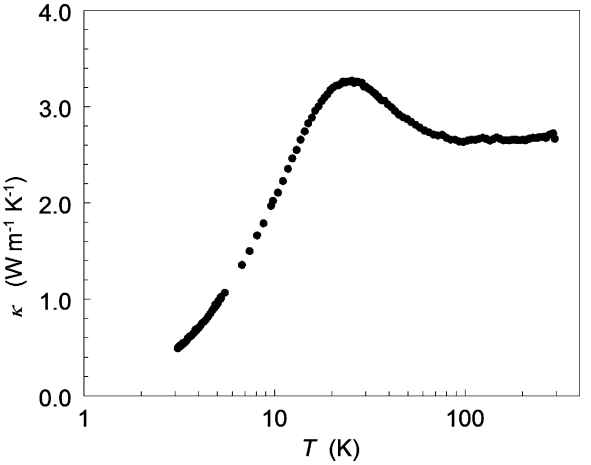

FIG. 2. The experimentally determined thermal conductivity κ along the [110] direction of a single crystal of pure $Y_2Ti_2O_7$ as a function of temperature.

The thermal conductivity of a single crystal of the other pure titanate $Y_2Ti_2O_7$ aligned along the [110] lattice vector, also was determined. Figure 2 shows the results over the temperature range 3 to 300 K, which again follow the same characteristic pattern of thermal conductivity for crystalline insulating solids over this temperature range.[14,23,24] The values for $T > 80$ K are within 3% of our previously published values for $Y_2Ti_2O_7$,[26] but the present values are about 20% lower at the peak. Note that the value of the thermal conductivity at the peak is not so much an intrinsic property of the system but more of a reflection of sample quality. Our samples are very high-purity single crystals, so very small changes in purity or sample quality can significantly influence the maximum thermal conductivity. Although the earlier data also were for high-purity single crystals, the crystal alignment of that sample was not determined (and the sample is now degraded), so the present data $Y_2Ti_2O_7$ are used for direct comparison with this $(Er_{1-x}Y_x)_2Ti_2O_7$ series.

The thermal conductivities of four single crystals of the general formula $(Er_{1-x}Y_x)_2Ti_2O_7$ also were determined. Prior to measurement, the exact compositions were determined by electron microprobe analysis. The Er contents in percent, based on full occupancy of the A sites, were found to be 96.9 ± 0.7, 91.5 ± 0.3, 81.7 ± 0.4, and 52.9 ± 0.6, with each composition based on at least 20 electron microprobe measurements. The thermal conductivity results with varying x are shown in Fig. 3, along with the average thermal conductivity of the two single crystals of pure $Er_2Ti_2O_7$ and the thermal conductivity of the single crystal of pure $Y_2Ti_2O_7$ for comparison.

The thermal conductivities of the $(Er_{1-x}Y_x)_2Ti_2O_7$ solid solution single crystals generally drop as x increases to its highest value of 0.471. This drop is not unexpected due to the increasing influence of scattering by the dopant, shortening the phonon mean free path, and hence lowering the thermal conductivity. At high temperatures (~300 K) the thermal conductivities of all the samples, both pure and doped, appear to approach the approximate same value. The similarity of the

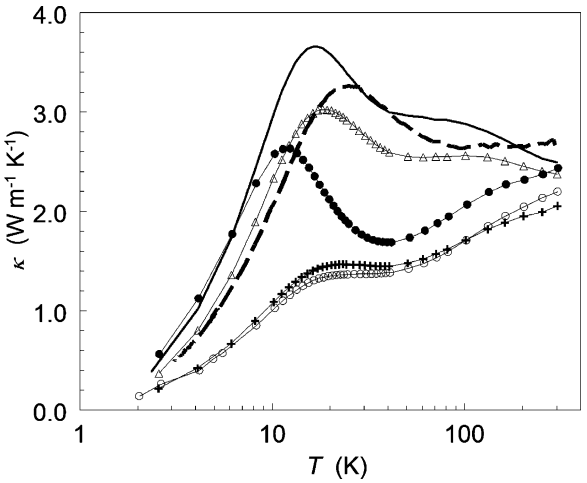

FIG. 3. The experimental thermal conductivities κ for high-purity single crystals of $(Er_{1-x}Y_x)_2Ti_2O_7$: Δ, $x = 0.031$; •, $x = 0.085$; +, $x = 0.183$; ○, $x = 0.471$. (Lines are guides for the eye.) Also shown for comparison are the values of κ for the single crystal of $Y_2Ti_2O_7$ (- - -) and the average values of κ for the two single-crystal $Er_2Ti_2O_7$ samples (——). All thermal conductivities were measured along the [110] direction.

thermal conductivity of the doped and pure compounds is the result of the greater importance of Umklapp scattering, relative to impurity scattering, at high temperatures.[14] This effect is highlighted in Fig. 4, which shows the thermal conductivity as a function of composition at various temperatures. In general, the thermal conductivity drops as x increases and then rises again at $x = 1$ (pure $Y_2Ti_2O_7$). (One exception to the general trends with temperature and composition is the $x = 0.085$ sample which has higher thermal conductivity at the lowest and highest temperatures measured, but follows the general trends at intermediate temperatures, $10 \leqslant T \leqslant 200$ K.) The thermal conductivity at 303 K shows the least variation across the compositional range [but similar in magnitude to the $(La_{1-x}Gd_x)_2Zr_2O_7$ system[13]] when compared to the thermal

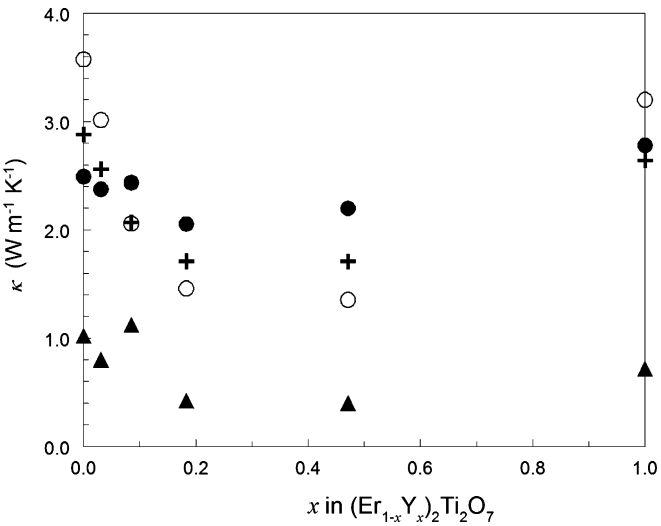

FIG. 4. The thermal conductivity κ as a function of the composition of single crystals of $(Er_{1-x}Y_x)_2Ti_2O_7$ at four different temperatures: •, 303 K; +, 101 K; ○, 20 K; ▲, 4 K.

conductivity at 101 and 20 K. At very low temperatures (4 K) the thermal conductivity again is more consistent across all compositions, with the exception of $x = 0.085$.

B. Minimum thermal conductivity, κ_{min}

At sufficiently high temperatures, the crystal structure becomes fully populated with phonons, and phonon-phonon interactions cause the phonon mean free path to be as short as possible.[27] In this temperature range the heat capacity and speed of sound are virtually independent of temperature and thus the thermal conductivity exhibits a high-temperature minimum κ_{min}. The value of κ_{min} has been modeled in two distinct manners.[27,28]

Clarke assumed the minimum phonon mean free path to be the cube root of the volume of one molecular unit and used the value of Young's modulus and density of the material in question to approximate the average phonon speed. By homogenizing all atoms in this model as having a mass M, equal to the weighted averages of the masses of the atoms in a unit cell, the minimum thermal conductivity at high temperature is given by

$$\kappa_{min} = 0.87 k_B N_A^{2/3} \frac{n^{2/3} \rho^{1/6} E^{1/2}}{M^{2/3}}, \qquad (2)$$

where k_B is Boltzmann's constant, N_A is Avogadro's number, n is the number of atoms per unit cell, ρ is the density of the material, and E is the Young's modulus.[27] In the present study, values for E, ρ, and M for the solid solutions were calculated as averages of the values for the pure compounds, weighted by their exact compositions. Literature values of the Young's moduli for $Er_2Ti_2O_7$ and $Y_2Ti_2O_7$ were used.[29,30]

A different minimum thermal conductivity model proposed by Cahill and Pohl considers the thermal conductivity within the Debye model, with the assumption that the scattering length is one half of the wavelength.[31] The expression for κ_{min} is based on the random walk between Einstein oscillators of varying sizes and can be calculated for each of the transverse and longitudinal polarizations v_i as follows:[31]

$$\kappa_{min} = \frac{1}{2.48} k_B n^{2/3} v_i 2 \left(\frac{T}{\theta_D^e}\right)^2 \int_0^{\theta_D^e} \frac{x^2 e^x}{(e^x - 1)^2} dx, \qquad (3)$$

where n is now the number density (number of atoms per unit volume), and θ_D^e is the *effective* Debye temperature, wherein all the lattice modes (3 acoustic and $3p - 3$ optical, with p atoms per unit cell) have been treated as Debye-like. The effective Debye temperature was calculated from the mean speed of sound as

$$\theta_D^e = \left(\frac{h}{2\pi k_B}\right) v_m (6\pi^2 n)^{1/3}. \qquad (4)$$

The total κ_{min} is the sum of the contributions from two transverse and one longitudinal mode. The transverse and longitudinal speeds of sound v_t and v_l, respectively, were calculated from the elastic constants $v_l = (c_{11}/\rho)^{1/2}, v_t = (c_{44}/\rho)^{1/2}$. The mean speed of sound v_m can be calculated from the transverse and longitudinal speeds of sound:

$$v_m = 3^{1/3}[(v_l)^{-3} + 2(v_t)^{-3}]^{-1/3}. \qquad (5)$$

TABLE I. The minimum thermal conductivities of $Er_2Ti_2O_7$, $Y_2Ti_2O_7$, and four doped compounds calculated using both the Clarke model[27] and the Cahill and Pohl[31] model.

Compound	Clarke model[27] (κ_{min}/WK^{-1}m^{-1})	Cahill and Pohl model[31] $T = 300$ K (κ_{min}/WK^{-1}m^{-1})
$Er_2Ti_2O_7$	1.03	1.46
$(Er_{0.969}Y_{0.031})_2Ti_2O_7$	1.03	1.47
$(Er_{0.915}Y_{0.085})_2Ti_2O_7$	1.06	1.48
$(Er_{0.817}Y_{0.183})_2Ti_2O_7$	1.07	1.49
$(Er_{0.529}Y_{0.471})_2Ti_2O_7$	1.11	1.54
$Y_2Ti_2O_7$	1.24	1.63

For the calculation of κ_{min} the elastic constants of $Y_2Ti_2O_7$ are available only from theory.[32] The $Er_2Ti_2O_7$ elastic constants were not available experimentally or theoretically, so they were estimated by extrapolating the theoretical c_{11} and c_{44} values for $Y_2Ti_2O_7$ and $La_2Ti_2O_7$[32] using relative molar masses. The estimate of v_m for $Er_2Ti_2O_7$ from extrapolation (5509 ms^{-1}) is very similar to the value calculated from Young's modulus[29] and the crystal density $v_m = (E/\rho)^{1/2} = 5490$ ms^{-1}, adding support for this approach.

Table I shows the values of the minimum thermal conductivity for $Er_2Ti_2O_7$, $Y_2Ti_2O_7$, and the four solid solutions, calculated using both the Clarke and the Cahill and Pohl models for minimum thermal conductivity.

Both models yield similar values of the minimum thermal conductivity at high temperature, but the Cahill and Pohl model yields higher values than the Clarke model for all the compositions. In both models, pure $Y_2Ti_2O_7$ has the highest κ_{min}, and $Er_2Ti_2O_7$ has the lowest κ_{min}. The experimental thermal conductivities show the same trend at $T = 300$ K, that is, the thermal conductivity of $Y_2Ti_2O_7$ is higher than $Er_2Ti_2O_7$. However, the experimental $T = 300$ K thermal conductivities of $Er_2Ti_2O_7$ and $Y_2Ti_2O_7$ are significantly higher than these κ_{min} values, indicating that these compounds need to be at a significantly higher temperature to reach their fully phonon-coupled minimum thermal conductivities. The values for κ_{min} of the doped compounds fall between the values of the pure titanates with the yttrium-rich compounds having the highest κ_{min}, as one would expect based on the calculated value of κ_{min} being higher for $Y_2Ti_2O_7$ than for $Er_2Ti_2O_7$.

C. Effective phonon mean free path

Dopant ions scatter phonons, and thus lower thermal conductivity by shortening the phonon mean free path. To observe this effect more directly, the effective phonon mean free paths of both the pure and doped titanates were calculated using Eq. (1). We refer to this as an "effective" mean free path because the model ignores dispersion and thereby could underestimate the mean free path by an order of magnitude.[33] However, this is not a serious problem here because the most important information is the trend in mean free path as a function of temperature or composition. For this analysis, published values of heat capacity were used for $Y_2Ti_2O_7$ and $Er_2Ti_2O_7$.[26,34] Although heat capacity usually is an additive property given quite accurately by the rule-of-mixtures, this system is an exception due to magnetic spin contributions which depend very strongly on the local environment, so we used the lattice contribution to the heat capacity[35] (derived from experimental heat capacity data) to determine phonon mean free paths for the solid solutions and the pure components. Using the Young's moduli for the pure titanates and measured densities, the speeds of sound in the pure materials were approximated by[24]

$$v = \sqrt{\frac{E}{\rho}}. \tag{6}$$

The speeds of sound of the solid solutions were approximated as weighted averages of the values for the pure compounds.

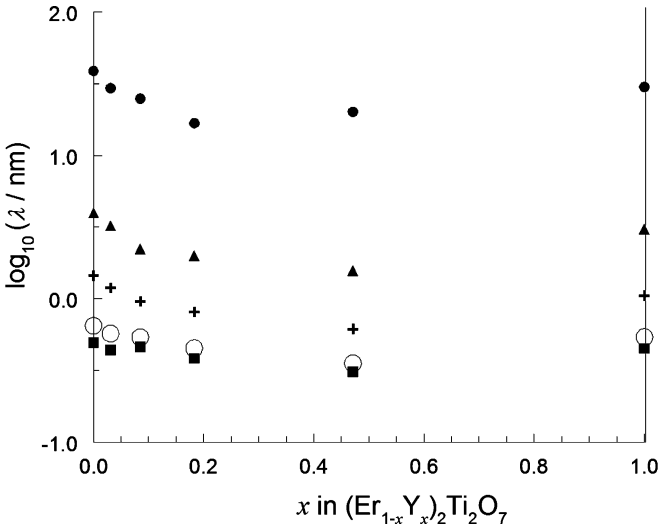

FIG. 5. The effective phonon mean free path λ in $\log_{10}$ form, as a function of the composition at various temperatures: •, $T = 20$ K; ▲, $T = 50$ K; +, $T = 100$ K; ○, $T = 200$ K; ■, $T = 300$ K.

Figure 5 shows the effective phonon mean free path (in $\log_{10}$ form) as a function of composition at various temperatures. Throughout this temperature range the pure titanates have longer phonon mean free paths than the doped compounds. This was the expected result as the dopants act as point defects. The doped compounds with higher concentrations of Y^{3+} ions ($x = 0.183$ and $x = 0.471$) have shorter phonon mean free paths than the doped compounds with a lower concentration of Y^{3+} ions ($x = 0.031$ and $x = 0.085$). At $T = 20$ K, pure $Er_2Ti_2O_7$ and pure $Y_2Ti_2O_7$ both have much longer effective phonon mean free paths than the solid solutions, but at 300 K, the differences are smaller.

If the total (not just lattice) heat capacity is used for the mean free path calculation from Eq. (1), below about 10 K the effective phonon mean free paths of the two parent compounds $Er_2Ti_2O_7$ and $Y_2Ti_2O_7$ behave very differently. The phonon mean free path of $Y_2Ti_2O_7$ increases with decreasing temperature, as usual for simple crystalline solids. However, the effective phonon mean free path based on total heat capacity of $Er_2Ti_2O_7$ deviates from the expected pattern and only increases with decreasing temperature down to about 6 K and then falls as the temperature is lowered further. This anomalous behavior

is due to a magnetic transition which occurs at low temperature in $Er_2Ti_2O_7$,[34] associated with the paramagnetic Er^{3+} ions in the pyrochlore lattice.[36] The magnetic transition causes a significant increase in heat capacity at very low temperature,[34] but there is no corresponding anomaly in the thermal conductivity, and thus a low-temperature peak in the total-heat-capacity-based effective phonon mean free path is observed. However, if only the lattice contribution to the heat capacity is considered (as for the data shown in Fig. 5), the temperature dependence of the mean free path of $Er_2Ti_2O_7$ is similar to diamagnetic $Y_2Ti_2O_7$. At low temperatures the doped compounds also show anomalous mean free path behavior as for $Er_2Ti_2O_7$, due to the presence of paramagnetic Er^{3+} ions. However, the magnetic behavior only contributes in a major way to the phonon mean free path at very low temperatures.

IV. CONCLUSIONS

Schelling's theoretical studies suggest that *A*-site doping with a lighter ion has only a small effect on thermal conductivity due to the competing factors of dopant ions acting as point defects and an increase in thermal conductivity due to the presence of these lighter atoms.[13] Our investigations of the effect of doping of $Er_2Ti_2O_7$ with Y^{3+} ions on thermal conductivity is analogous to the situation Schelling described because Y^{3+} is the same size as Er^{3+} but significantly less massive, and the theoretical high-temperature value of κ_{min} of pure $Y_2Ti_2O_7$ is higher than that of $Er_2Ti_2O_7$. We rule out the influences of sample purity, crystal quality, anisotropy, and the need for other properties to derive thermal conductivity by directly measuring the thermal conductivities of high-quality single crystals, aligned along the [110] direction. We observed that the thermal conductivity of $Y_2Ti_2O_7$ is higher than that of $Er_2Ti_2O_7$ at $T = 300$ K, but the opposite is true from 20 to 200 K. Furthermore, the significant decrease in thermal conductivity that we observe upon doping $Er_2Ti_2O_7$ with Y^{3+} ions shows definitively that, in the temperature range from about 2 to 300 K, the impurity scattering effect of the lighter Y^{3+} ions is the predominant limiter of the thermal conductivity. This conclusion is supported by the finding that the phonon mean free path of the doped compounds decreases with increased dopant concentrations. This information can be used to tailor thermal conductivity over a wide range of values.

ACKNOWLEDGMENTS

We gratefully acknowledge the assistance of Professor T. S. Cameron in aligning the crystals, A. George in cutting the crystals, D. MacDonald for electron microprobe work, and P. Scallion for EDS analysis. This work was supported by NSERC of Canada, and facilities used at McMaster's Brockhouse Materials Research Institute and Dalhousie's Institute for Research in Materials were supported by the Canada Foundation for Innovation and NSERC.

*Corresponding author: mary.anne.white@dal.ca

[1] M. A. Subramanian, G. Aravamudan, and G. V. Subba Rao, Prog. Solid State Chem. **15**, 55 (1983).
[2] G. R. Lumpkin, M. Pruneda, S. Rios, K. L. Smith, K. Trachenko, K. R. Whittle, and N. J. Zaluzec, J. Solid State Chem. **180**, 1512 (2007).
[3] J. E. Greedan, J. Alloys Compd. **408**, 444 (2006).
[4] P. K. Schelling, S. R. Phillpot, and R. W. Grimes, Philos. Mag. Lett. **84**, 127 (2004).
[5] J. Feng, B. Xiao, C. L. Wan, Z. X. Qu, Z. C. Huang, J. C. Chen, R. Zhou, and W. Pan, Acta Mater. **59**, 1742 (2011).
[6] J. S. Tse and M. A. White, J. Phys. Chem. **92**, 5006 (1988).
[7] L. Qiu, M. A. White, Z. Li, J. S. Tse, C. I. Ratcliffe, C. A. Tulk, J. Dong, and O. F. Sankey, Phys. Rev. B **64**, 024303 (2001).
[8] C. A. Kennedy and M. A. White, Solid State Commun. **134**, 271 (2005).
[9] C. A. Kennedy, M. A. White, A. P. Wilkinson, and T. Varga, Appl. Phys. Lett. **90**, 151906 (2007).
[10] M. R. Winter and D. R. Clarke, J. Am. Ceram. Soc. **90**, 533 (2007).
[11] C. L. Wan, W. Pan, Q. Xu, Y. X. Qin, J. D. Wang, Z. X. Qu, and M. H. Fang, Phys. Rev. B **74**, 144109 (2006).
[12] W. Pan, C. L. Wan, Q. Xu, J. D. Wang, and Z. X. Qu, Thermochim. Acta **455**, 16 (2007).
[13] P. K. Schelling, Comput. Mater. Sci. **48**, 336 (2010).
[14] R. Berman, *Thermal Conduction in Solids* (Oxford University Press, Oxford, 1976).
[15] O. Knop, F. Brisse, and L. Castelliz, Can. J. Chem. **47**, 971 (1969).
[16] R. D. Shannon, Acta Crystallogr. Sect. A **32**, 751 (1976).
[17] J. S. Gardner, B. D. Gaulin, and D. McK. Paul, J. Cryst. Growth **191**, 740 (1998).
[18] H. A. Dąbkowska and A. B. Dąbkowski, "Crystal Growth of Oxides by Optical Floating Zone Technique. Experimental Approach to Defects Determination" in *Springer Handbook of Crystal Growth, Defects and Characterization* (Springer, Berlin, 2009).
[19] *PPMS Hardware and Options Manual*, 3rd ed. (Quantum Design, San Diego, CA, 2002).
[20] L. C. K. Carwile and H. J. Hoge, *Thermal Conductivity of Pyrex Glass: Select Values* (United States Army, Natick Laboratories, Natick, 1966).
[21] M. J. Assael, K. Gialou, K. Kakosimos, and I. Metaxa, Int. J. Thermophys. **25**, 397 (2004).
[22] See Supplemental Material at http://link.aps.org/supplemental/10.1103/PhysRevB.86.054303 for tables of thermal conductivity data.
[23] T. M. Tritt, *Thermal Conductivity: Theory, Properties, and Applications* (Kluwer Academic/Plenum Publishers, New York, 2004).
[24] M. A. White, *Physical Properties of Materials* (CRC, Boca Raton, FL, 2012).
[25] P. G. Klemens, High Temp. High Press. **23**, 241 (1991).
[26] M. B. Johnson, D. D. James, A. Bourque, H. A. Dąbkowska, B. D. Gaulin, and M. A. White, J. Solid State Chem. **182**, 725 (2009).
[27] D. R. Clarke, Surf. Coat. Technol. **163**, 67 (2003).
[28] D. G. Cahill, S. K. Watson, and R. O. Pohl, Phys. Rev. B **46**, 6131 (1992).

[29]M. P. van Dijk, K. J. de Vries, and A. J. Burggraaf, Solid State Ionics **9&10**, 913 (1983).
[30]Y. Jiang, J. R. Smith, and G. R. Odette, Acta Mater. **58**, 1536 (2010).
[31]D. G. Cahill and R. O. Pohl, Annu. Rev. Phys. Chem. **39**, 93 (1988).
[32]J. M. Pruneda and E. Artacho, Phys. Rev. B **72**, 085107 (2005).
[33]G. Chen, Int. J. Therm. Sci. **39**, 471 (2000).
[34]J. P. C. Ruff, J. P. Clancy, A. Bourque, M. A. White, M. Ramazanoglu, J. S. Gardner, Y. Qiu, J. R. D. Copley, M. B. Johnson, H. A. Dąbkowska, and B. D. Gaulin, Phys. Rev. Lett. **101**, 147205 (2008).
[35]M. A. White *et al*. (unpublished).
[36]J. S. Gardner, M. J. P. Gringras, and J. E. Greedan, Rev. Mod. Phys. **82**, 53 (2010).